

BoxFusion: Reconstruction-Free Open-Vocabulary 3D Object Detection via Real-Time Multi-View Box Fusion

Yuqing Lan¹ Chenyang Zhu¹ Zhirui Gao¹ Jiazhao Zhang³ Yihan Cao¹

Renjiao Yi¹ Yijie Wang^{1†} Kai Xu^{1,2†}

¹National University of Defense Technology ²Xiangjiang Laboratory ³Peking University

Abstract

Open-vocabulary 3D object detection has gained significant interest due to its critical applications in autonomous driving and embodied AI. Existing detection methods, whether offline or online, typically rely on dense point cloud reconstruction, which imposes substantial computational overhead and memory constraints, hindering real-time deployment in downstream tasks. To address this, we propose a novel reconstruction-free online framework tailored for memory-efficient and real-time 3D detection. Specifically, given streaming posed RGB-D video input, we leverage Cubify Anything as a pre-trained visual foundation model (VFM) for single-view 3D object detection by bounding boxes, coupled with CLIP to capture open-vocabulary semantics of detected objects. To fuse all detected bounding boxes across different views into a unified one, we employ an association module for correspondences of multi-views and an optimization module to fuse the 3D bounding boxes of the same instance predicted in multi-views. The association module utilizes 3D Non-Maximum Suppression (NMS) and a box correspondence matching module, while the optimization module uses an IoU-guided efficient random optimization technique based on particle filtering to enforce multi-view consistency of the 3D bounding boxes while minimizing computational complexity. Extensive experiments on ScanNetV2 and CA-1M datasets demonstrate that our method achieves state-of-the-art performance among online methods. Benefiting from this novel reconstruction-free paradigm for 3D object detection, our method exhibits great generalization abilities in various scenarios. The code will be released at [project page](#).

1. Introduction

Recently, embodied intelligence has attracted great interest, with many well-developed applications, such as embodied

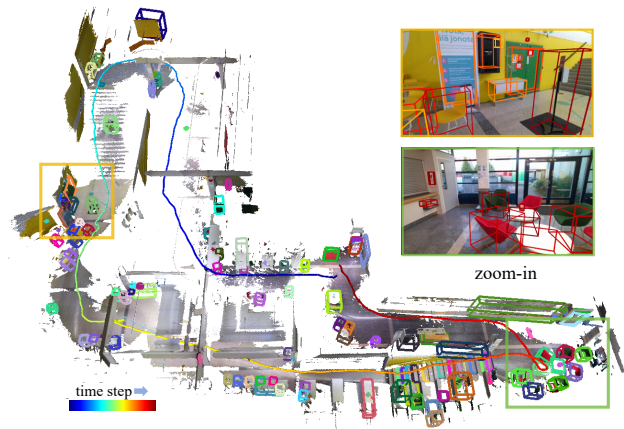


Figure 1. The state-of-the-art method leverage dense reconstruction for online 3D perception. Our method is reconstruction-free, which can efficiently perform fine-grained 3D object detection with open-vocabulary semantics with over 20 FPS and 7GB GPU memory usage even in a multi-floor building (over 1000m²). Note that the reconstructed mesh is only for visualization here.

navigation [2, 42, 46], mobile manipulation [39, 45]. These embodied applications are mainly based on scene understanding (e.g., 3D object detection [28, 29], semantic segmentation [9, 22], and depth estimation [17, 40]). Current methods all reconstruct the scene first for scene understanding with dense representations, such as point clouds[24], voxels[47], etc. However, we found that a sparse representation of reality, which only preserves the position, scale, and semantics of objects' bounding boxes, as a scene representation, is sufficient to complete the downstream tasks, such as scene graph generation [12] and collision detection [33].

Primary research in 3D object detection has focused predominantly on representations of 3D point clouds or meshes in the past. As inputs to these methods, point clouds inevitably undergo sparsification operations for computational feasibility, which introduce detection deficiency caused by lower resolution. Learning-based methods aim

[†]Corresponding authors

to incorporate inductive biases into models to mitigate this issue [5, 24, 28]. Yet, the substantial discrepancy between 3D representations and physical reality restricts their applicability primarily to large, prominent objects. Therefore, some point-based methods [25] have attempted to use images as auxiliary inputs to enhance the performance. Recently, with the development of visual foundation models (VFM) [10, 19, 27], researchers have started to leverage VFMs to incorporate rich semantic information from 2D images into point cloud-based methods, enabling open-vocabulary detections [1, 7, 21]. While these methods are still dependent on dense point cloud reconstruction, which is prone to being affected by noise (e.g., accumulated errors in the reconstruction or noise in the sensors) or storage limitations of large-scale scenarios. Furthermore, these methods typically follow a two-stage paradigm that requires complete dense point cloud reconstruction as inputs, which significantly hinder real-time applications. To address these challenges, some recent works have explored online perception methods. These methods either introduce a memory adapter [38] to store the reconstructed point cloud or utilize 2D foundational models to extract fine-grained object masks and semantics from each view and then fuse them with the reconstructed dense point cloud for open-vocabulary perception [31, 37]. However, these online perception methods still rely on dense point-cloud reconstruction as input, which significantly increases computational overhead and degrades real-time performance, making it difficult to meet the requirements of real-time interaction in many downstream tasks.

To overcome these challenges, in this work, we propose a novel reconstruction-free online framework specifically designed for memory-efficient and real-time open-vocabulary 3D object detection. Our approach is inspired by many embodied tasks, such as navigation and manipulation, which do not require a complete reconstruction of the scene but rather focus on detecting and understanding the objects within it. As shown in Figure 1, by eliminating the need for dense point-cloud reconstruction, we can achieve faster and more efficient 3D object detection while maintaining high accuracy. Specifically, for streaming RGB-D video input, we leverage Cubify Anything [14] as a pre-trained visual foundation model (VFM) for efficient single-view 3D object proposal generation. These proposals are enriched with open-vocabulary semantics by using CLIP [27] to extract the semantic feature of the detected instance. An association module then aggregates multi-view proposals corresponding to the same instance through 3D Non-Maximum Suppression (NMS) and 2D box correspondence matching. Since the proposals from Cubify Anything are local and view-specific, it is of great necessity to aggregate and optimize the associated proposals from different views of the same object. Therefore, to further en-

hance multi-view consistency, we employ an optimization module, an IoU-guided efficient random optimization technique, which is grounded by particle filtering to overcome the highly non-linear optimization of object boxes. In this way, we can enforce multi-view consistency of the proposals of 3D bounding boxes while minimizing computational complexity to achieve real-time 3D object detection.

Extensive experiments on the CA-1M and ScanNetV2 datasets demonstrate that our method achieves state-of-the-art performance among online open-vocabulary 3D detection methods. Benefiting from its reconstruction-free paradigm, our approach exhibits exceptional generalization capabilities and enables real-time performance even in large-scale environments exceeding 1000 square meters, paving the way for the deployment in large-scale and challenging scenarios. In summary, our contributions are as follows:

- We propose a novel reconstruction-free paradigm for online open-vocabulary 3D object detection, which models structural object layouts with desirable running and memory efficiency.
- We propose a multi-view box fusion technique based on particle filtering using random optimization, enabling real-time and consistent 3D bounding box detection.
- We have implemented an efficient system of online open-vocabulary 3D object detection. Extensive experiments validate the superior performance and robustness of our method in various challenging scenarios.

2. Related Work

Traditional 3D object detection: Pioneered by PointNet [23], 3D object detection methods used to rely on dense labeled data corresponding to closed-set categories of objects. Point-based methods [20, 24, 36] follow the feature extraction techniques used in 2D object detection, and extract permutation-invariant point cloud features by 3D backbones, coupled with 3D detection heads. The follow-up works [3, 6, 13] boost the performance by incorporating graph neural networks, better proposal generation, and contextual information. backbones like Voxel-based methods [28, 29, 47], akin to 2D detection, convert point clouds into regular grids, equipped with 3D convolutional neural networks (CNNs) for feature extraction. Favorable detection on notable room-level objects (e.g., chairs and tables), but poor generalization on objects of unseen categories probably hinders the applications on more complicated tasks.

Open-vocabulary 3D object detection: With the development of visual foundation model (VFM) like SAM [10] or DINO [19], recent works [7, 21, 35] first establish the correspondence between 3D data like point clouds and 2D RGB images, and subsequently employ vision-language model (VLM) like CLIP [30] to segment images for more fruitful

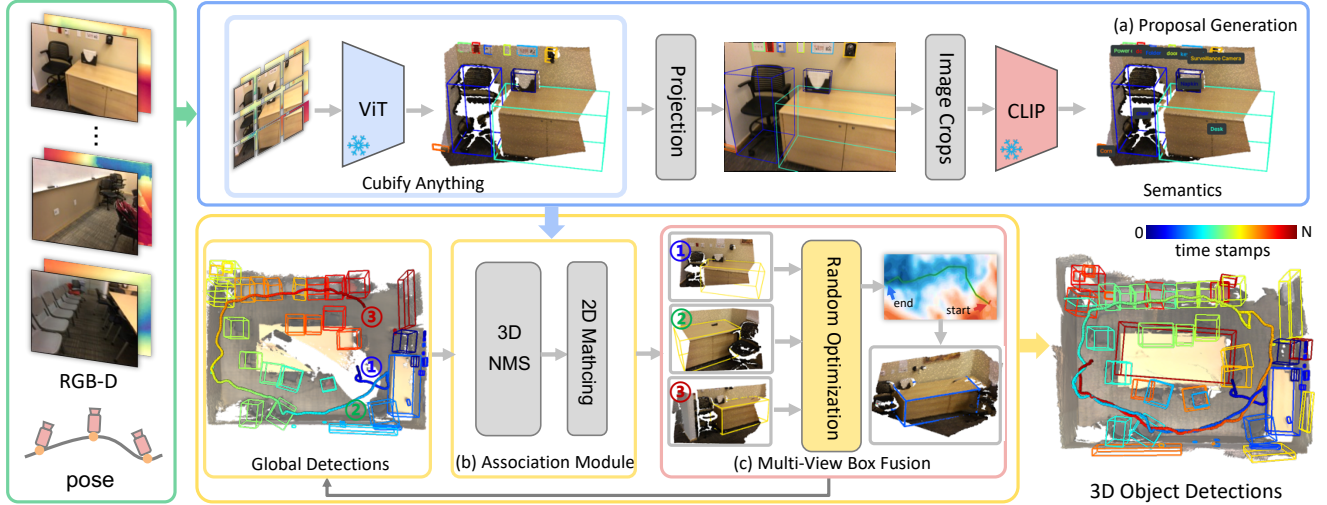


Figure 2. Method Overview of BoxFusion. (a) Given online RGB-D images with camera poses, we use Cubify Anything to generate bounding box proposals for each keyframe, and back-project them to image planes to get the image crops to obtain the open-vocabulary semantics with CLIP. (b) We employ an association module to perform 3D NMS for global boxes with proposals from the new keyframe, removing redundant boxes and associating those belonging to the same object. (c) With the associated candidate boxes of an object, we adopt random optimization based on particle filtering to fuse these candidate boxes into a multi-view consistent one using the IoU of the convex hulls of projected box corners. (e.g., there are three boxes for the highlight desk at three timestamps that only cover a part of it, and the boxes are not accurate enough). In this way, our method can efficiently detect fine-grained objects in real time without reconstruction.

object proposals and corresponding semantics. These methods demonstrate improvements in detecting objects of novel categories in 3D scenes and make cross-modal retrieval between images and text descriptions feasible. However, these methods still rely on 3D data like point clouds as the core representation, which often suffers from the relatively poor resolution of point clouds and limits the flexibility with high computational overheads. SpatialLM [32] encodes the reconstructed point cloud and detects all the objects queried by a designed text prompt. Another paradigm is to leverage the 2D image features for 3D object detection, predicting the 3D bounding box directly. Cubify Anything [14] predicts metric fine-grained 3D bounding boxes by using a novel large-scale dataset and Encoder-Decoder vision transformer (ViT). DetAny3D [43] proposes a novel 3D detection framework that directly predicts 3D bounding boxes for a single image, leveraging the rich image features from VFM. However, these methods are primarily designed for single-view 3D object detection and exhibit limited generalization capabilities in dynamic online scanning scenarios.

Online 3D perception: Online 3D perception is a crucial task in robotics, enabling real-time scene understanding towards the surrounding environments. [38] employs a memory-based adapter for online 3D perception, including semantic and instance segmentation and 3D object detection. However, it is limited to closed-set categories and does not support open-vocabulary detection. Recent works [31, 37, 41] exploit the potential of 2D VFM like SAM [10] or

CropFormer [26] for online 3D instance segmentation via per-frame mask merging. However, multi-view fusion relying on 3D data representations (e.g., point clouds) inherently introduces sparsification artifacts and sensor-induced noise during reconstruction (e.g., depth holes from invalid measurements). Consequently, methods dependent on reconstructed point clouds to determine the spatial overlap of different masks are fragile, especially for small objects. Moreover, maintaining a dense 3D structure increases the computational overhead, and methods that rely on reconstructed point clouds to determine the spatial overlap of different masks are fragile, especially for small objects. Maintaining a dense 3D structure increases the computational overhead and reduces the running and memory efficiency in terms of online settings and larger-scale scenarios. Compared to these methods, our method is reconstruction-free and more efficient in diverse scenarios.

3. Methodology

In this section, we first introduce the overall pipeline of our method. The insight of our method is to leverage foundation models to generate single-view fine-grained 3D bounding boxes and fuse them into multi-view consistent global 3D bounding boxes. In this way, the proposed reconstruction-free pipeline is able to generate scene-level 3D bounding boxes of fine-grained objects.

3.1. Overview

As shown in Figure 2, our method consists of three main components: single-view prediction, box association, and box fusion. Given RGB-D posed images as inputs, we first predict single-view 3D bounding box proposals using Cubify Anything [14] for each keyframe, and transform the boxes from camera to world coordinates. These 3D proposals are then projected back to 2D in order to crop the images and use CLIP [27] for semantic features. To associate the candidate boxes of the same instance, we first use 3D NMS to filter spatially overlapping boxes, coupled with a 2D correspondence matching module to associate small objects, since proposals of small objects are more likely to be adjacent but not close enough to have overlaps. Finally, we fuse these proposals into a single global 3D bounding box for each object in the scene. Specifically, inspired by [44], we employ the IoU-guided random optimization equipped with a pre-sampled particle swarm templates (PST) for better on-line efficiency and robustness to the highly-nonlinear optimization of box fusion. By this means, the proposed method is real-time and efficient for fine-grained scene-level 3D bounding box generation.

3.2. Proposal Generation

In the era of foundation models, 3D object detection has been significantly boosted by leveraging large-scale pre-trained models. In this work, we adopt Cubify Anything [14] for fine-grained box proposal generation. Cubify Anything is a state-of-the-art method that can generate 3D bounding boxes from a single RGB-D image, and it is trained on a large-scale dataset with exhaustive objects.

To be specific, given the successive RGB-D inputs $\{(I_t, D_t)\}_{t=1}^N$ with N images in total, where I_t is the RGB frame and D_t is the depth frame, we first obtain M 3D bounding box proposals $\{\bar{B}_t^i\}_{i=1}^M$ for each image using Cubify Anything. Each box \bar{B}_t^i is represented in the camera coordinate system. To transform the boxes to the world coordinate system, we apply the camera pose transformation \mathcal{T}_t to each box \bar{B}_t^i , and obtain the global 3D boxes $\{\mathcal{G}_t^i\}_{i=1}^M$. In order to obtain the boxes with the corresponding semantics, we project the 3D boxes back to the 2D image planes I_t and crop the corresponding image regions according to the projected box corners. The cropped images are then fed into a pre-trained CLIP model Θ [27] to obtain the semantic features $\{F_i\}_{i=1}^N$ of each box proposal as shown in Eq. 1.

$$F_t^i = \Theta(P(I_t, K_t, \{\bar{B}_t^i\})), \quad (1)$$

where K_t denotes the camera intrinsics and P indicates the projection and image cropping operation.

3.3. Association Module

In this section, we introduce the box association module to associate the 3D bounding boxes of the same instance

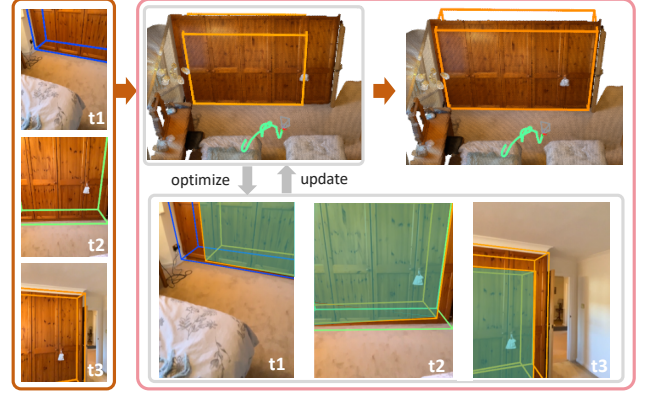


Figure 3. Visualization of multi-view box fusion using random optimization with the IoU of the intersecting projected convex hulls between the global box and single-view proposals. Three single-view proposals of a cabinet (bottom) are fused into a global one (top).

across different views. The association is crucial for maintaining consistent global 3D bounding boxes since numerous bounding boxes are generated from each single view. The spatial association and correspondence association are introduced as follows.

3.3.1. Spatial Association

Previous methods [31, 37] mainly exploit spatial overlap for association, which is valid for most room-level common objects like chairs and desks, but can not generalize to small objects (e.g., a TV remote on the table). The reason is that proposals for most small objects generated from different methods are usually adjacent but not spatially overlapped, which may result in the ignorance of detection for small objects. To address this challenge, we propose a novel two-stage association module: 3D Non-Maximum Suppression (NMS) for associating spatially overlapping boxes, and a 2D correspondence matching module for associating the remaining boxes, which are designed to associate fine-grained objects.

Concretely, given the local box proposals B_t^i , we add these to global bounding boxes \mathcal{G}_{t-1} and form current global boxes \mathcal{G}_t at the frame t . We need to determine whether any of the global boxes correspond to the other and remove the redundant ones. Compared to the axis-aligned NMS used in previous methods [20, 24], we aim to generate scene-level oriented 3D bounding boxes. Therefore, we adopt the NMS for oriented bounding boxes. To be specific, we first sort \mathcal{G}_t by the corresponding scores from Section 3.2. For each box \mathcal{G}_t^i indexed by the descending order of scores, we calculate the IoU between \mathcal{G}_t^i and the other boxes in \mathcal{G}_t . The IoU is calculated based on the convex hull of the 3D bounding boxes, which is more suitable for oriented boxes.

For online efficiency, we uniformly sample O_n points in the convex hull of each pair of 3D bounding boxes, and only those that are likely to have overlap are considered by checking if the points on the edges are included in each other. For a pair of 3D bounding boxes \mathcal{B}_i and \mathcal{B}_j ($i > j$ in the descending order of scores), the 3D convex-based IoU Ω_{ij} is defined as Eq. 2. We manage a candidate list Ψ for all global boxes \mathcal{G}_t . We filter \mathcal{B}_j if Ω_{ij} is higher than the threshold τ_{3d} and \mathcal{B}_j is then associated with \mathcal{B}_i if the camera direction is larger than τ_r or the camera translation is larger than τ_t compared to all candidate boxes in Ψ_i .

$$\Omega_{ij} = \frac{\sum_{k=1}^{O_n} \mathcal{C}(O_k, \mathcal{B}_i \cup \mathcal{B}_j)}{\sum_{k=1}^{O_n} \mathcal{C}(O_k, \mathcal{B}_i) + \sum_{k=1}^{O_n} \mathcal{C}(O_k, \mathcal{B}_j)}, \quad (2)$$

where \mathcal{C} is the indicator function that returns 1 if the point $O_k \in \mathcal{B}_i$, otherwise 0 and $\mathcal{B}_i \cup \mathcal{B}_j$ denotes the union of convex hulls of 3D bounding box \mathcal{B}_i and \mathcal{B}_j .

3.3.2. Correspondence Association

While the spatial association can reliably associate room-level common objects, small objects are challenging to associate since proposals for the same object are less accurate and likely to be spatially adjacent but not overlapping. Inspired by [16, 34], we argue that image-based correspondences are efficient and robust to match box proposals from different camera views that belong to the same object instance. However, directly using pre-trained models to find correspondence between the current image I_t and all historical frames that have visibility overlap is time-consuming and computationally expensive. Therefore, we propose a simple yet effective solution that projects the global 3D boxes \mathcal{G}_{t-1} at frame $t-1$ to the current image I_t , and determines whether the current candidate box \mathcal{B}_i corresponds to any global box in \mathcal{G}_{t-1} with M boxes in total by the IoU of projective bounding boxes as shown in Eq. 3.

$$j_{max} = \arg \max (\Phi(\mathcal{P}(T_t^{-1}, \mathcal{B}_i), \mathcal{P}(T_t^{-1}, \mathcal{G}_t^j))), j \in M, \quad (3)$$

where Φ denotes the 2D IoU of two convex hulls obtained from the projective corners of 3D bounding boxes. \mathcal{P} refers to the projection using the pin-hole camera assumption. If the IoU Φ_{ij} between the current candidate \mathcal{B}_i and global box $\mathcal{G}_t^{j_{max}}$ is larger than τ_{2d} , similar strategies in the spatial association are leveraged to determine whether \mathcal{B}_i should be added to the candidate list $\Psi_{j_{max}}$ for further multi-view box fusion.

3.4. Multi-view Box Fusion

Since the proposals from different camera views are local and not entirely accurate, it is of great necessity to fuse these candidate boxes belonging to the same object into a multi-view consistent bounding box. For example, the sequential

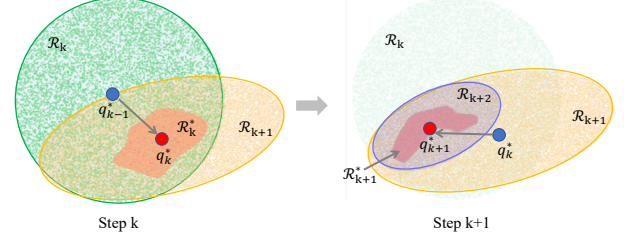


Figure 4. 2D example of particle filtering optimization (PFO) using pre-sampled swarm template (PST) for box fusion. At step k , particles in \mathcal{R}_k^* are selected as the superior set, moving the center q_{k-1}^* of particles \mathcal{R}_k to q_k^* and rescaling \mathcal{R}_k to \mathcal{R}_{k+1} . Similar moving and rescaling is employed to the particle set \mathcal{R}_{k+1} at step $k+1$. In this way, the optimization of box fusion can converge efficiently and accurately.

camera views only cover parts of a big cloth cabinet, and there would be several separate 3D boxes for the cabinet without box fusion.

As shown in Figure 3, for global 3D boxes \mathcal{G}_t^i and corresponding candidate box list Ψ_t^i , the goal is to aggregate the associated 3D boxes in Ψ_t^i and fuse them into a global one that is consistent in multiple views of Ψ_t^i . Empirically, we find the proposals generated by foundation models like Cubify Anything [14] look accurate in 2D images but are biased from the ground truth in 3D with scale uncertainty. Therefore, we propose to optimize the position and scales of the global box \mathcal{G}_t^i to fit the proposals Ψ_t^i in different views of the same object. Given the position $\mathbf{p} = (x, y, z)$ and shape $\mathbf{s} = (l, w, h)$ of \mathcal{G}_t^i , which are initialized as the average of those of boxes in Ψ_t^i , we aim to optimize the 6D variables $(\mathbf{p}, \mathbf{s}) = (x, y, z, l, w, h)$ to enable the global box \mathcal{G}_t^i to exactly cover each candidate box in the corresponding view.

Let us define the objective function first. The global box \mathcal{G}_t^i with parameters (\mathbf{p}, \mathbf{s}) to be optimized is projected to images $\{I_j | j \in \varphi_t^i\}$ with camera poses $\{T_j | j \in \varphi_t^i\}$, where φ_t^i is the set of camera indices of Ψ_t^i . The projected box corners of the global box \mathcal{G}_t^i in image I_j are used to derive a 2D convex hull denoted as α_{ij} . Similarly, we can obtain the candidate box 2D convex hull β_{ij} . The goal is to maximize the 2D IoU between α_{ij} and β_{ij} in each view. α_{ij} can be obtained by projecting the corners of \mathcal{G}_t^i to the image I_j using the camera pose T_j . The optimization can be formulated as follows:

$$\alpha_{ij} = \mathcal{P}(T_j^{-1}, (\mathcal{G}_t^i(\mathbf{p}, \mathbf{s}))). \quad (4)$$

$$(\mathbf{p}^*, \mathbf{s}^*) = \arg \max_{\mathbf{p}, \mathbf{s}} \sum_{j \in \varphi_t^i} \mathcal{H}(\alpha_{ij}, \beta_{ij}), \quad (5)$$

where \mathcal{H} is the 2D IoU function between two convex hulls.

The goal is to optimize the objective function in Eq. 5, but the optimization is highly non-linear and challeng-

ing to solve in real time. Inspired by [8, 44], to address this, we propose to use a *pre-sampled particle swarm template (PST)* to guide the optimization. This process is based on *particle filtering optimization (PFO)*, and the likelihood function corresponding to Eq. 5 can be formulated as 6.

$$p(g|\mathbf{p}, \mathbf{s}) = \exp \left(-\frac{1}{\xi} \sum_{j \in \varphi_t^i} \mathcal{H}(\alpha_{ij}, \beta_{ij}) \right), \quad (6)$$

where g denotes the observation function and ξ is a temperature.

The PST is a set of N_{pst} pre-sampled particles uniformly sampled in 6D space corresponding to the position $\mathbf{p} = (x, y, z), \mathbf{p} \in [-1, 1]$ and shape $\mathbf{s} = (l, w, h), \mathbf{s} \in [0, 1]$. With the initialized global box $\mathcal{G}_t^i(\mathbf{p}', \mathbf{s}')$, we add the PST to $\mathcal{G}_t^i(\mathbf{p}', \mathbf{s}')$ and detect which particle fits better using the objective function in Eq. 5. As shown in Figure 4, we select the best particles in \mathcal{R}_k as a superior set \mathcal{R}_k^* , which is moved and rescaled according to the superior set \mathcal{R}_k^* in step k . Then we can obtain the best transformation $q_k^* = (\mathbf{p}_k^*, \mathbf{s}_k^*)$, which are added to the current observation: $q' = (\mathbf{p}', \mathbf{s}') + (\mathbf{p}_k^*, \mathbf{s}_k^*)$. Once the iteration reaches the maximum number or the optimization converges, we use the current observation $(\mathbf{p}', \mathbf{s}')$ as the optimized one. Subsequently, we update the global box \mathcal{G}_t^i with the finally optimized parameters $q' = (\mathbf{p}', \mathbf{s}')$. The proposed random optimization is performed once the number of candidate boxes Ψ_t^i is larger than a threshold τ_{box} , or new candidates are added to the list.

4. Experiments

4.1. Experimental Setup

Datasets: We evaluate our method on the CA-1M [14] and ScanNetV2 [4] dataset. CA-1M is a large-scale dataset for class-agnostic 3D object detection with about 15M frames, including over 440K objects, which include lots of small but common objects in daily life. The ground truth 3D bounding boxes are labeled on the scan mesh from a FARO laser. There are 107 validation scenes in CA-1M. ScanNetV2 is a large RGB-D indoor dataset with a training set of 1201 scenes and a validation set of 312 scenes, which labels 18 categories of room-level objects.

Baselines: We mainly compare our methods to state-of-the-art offline point-cloud based methods: FCAF [28], TR3D [29] and SpatialLM [32]. Since there are no online open-vocabulary 3D detection alternatives, we take online perception methods: EmbodiedSAM [37] and OnlineAnySeg [31] into consideration, which are initially designed for instance segmentation and are post-processed for gravity-aware 3D bounding box detection.

Metrics: We use the standard metrics for 3D object detection following [1, 24], including Average Precision (AP)

at different IoU thresholds. For CA-1M and ScanNetV2, we report class-agnostic AP at IoU thresholds of 0.15, 0.25, and 0.5. ScanNetV2 only provides ground-truth axis-aligned bounding boxes, which requires results of all methods are axis-aligned for fair comparison. The running efficiency of the system FPS and GPU memory usage are considered as well.

Implementation Details: We evaluate RemixFusion on a desktop PC equipped with a 3.90GHz Intel Core i9-14900K CPU and an NVIDIA RTX 3090 Ti GPU. We implement the Iou-based random optimization based on the PyCUDA [11] libraries for acceleration. For the semantics of open-vocabulary categories, we use the text embedding of the provided categories (over 300) in [18] to match the detected objects. More details can be found in the supplementary materials. We highly recommend referring to supplementary videos for a more intuitive understanding of our method.

4.2. Quantitative Results

The quantitative comparison of our method and state-of-the-art baselines on CA-1M and ScanNetV2 is shown in Table 1. All sequences of the CA-1M validation set and eight sequences of ScanNetV2 are considered. Class-agnostic detection is adopted, since it is easier to obtain the categories of objects with the help of visual foundation models. Our method achieves the best performance on both datasets among the online methods, especially on CA-1M, where our method outperforms the second-best method by a large margin (22.05 improvement in AP_{15}). Point-based methods [28, 29, 32] demonstrate poor generalization on CA-1M, which is significantly lower than online alternatives in terms of AP_{15} to AP_{50} . The main reason is that point-based methods are trained on closed-set datasets, which focus on room-level object detection and typically ignore other ordinary and daily objects.

Online methods like EmbodiedSAM [37] and OnlineAnySeg [31] are designed for instance segmentation, and the results are transformed into bounding boxes for evaluation, following [15]. Details about the transformation are demonstrated in the supplementary materials. Online methods aim to detect objects with streaming RGB-D inputs, which overall shows better performance than offline methods. This may be attributed to that all online methods in Table 1 can efficiently capture the rich and useful contexts in images with VFMs for more comprehensive scene understanding.

Point-based method [28, 29] outperforms the others on ScanNetV2. These methods are trained on closed-set datasets and struggle to detect objects of other common categories, which is discussed in Section 4.3. AP_{15} of our method is over 30 on both CA-1M and ScanNetV2, demonstrating the robustness of our method. Moreover, the sig-

Method	Online	Open-Vocabulary	CA-1M			ScanNetV2			FPS
			AP_{15}	AP_{25}	AP_{50}	AP_{15}	AP_{25}	AP_{50}	
FCAF [28]	×	×	6.39	5.25	2.74	66.64	66.1	53.31	-
TR3D [29]	×	×	5.16	4.32	2.41	60.08	57.96	52.26	-
SpatialLM [32]	×	✓	1.40	0.78	0.15	8.06	4.04	0.58	-
EmbodiedSAM [37]	✓	×	9.17	5.01	0.80	5.22	2.46	0.33	10
OnlineAnySeg [31]	✓	✓	6.93	5.19	1.79	31.39	21.81	9.92	15
Ours	✓	✓	31.22	25.66	8.75	37.46	31.36	13.41	20

Table 1. Class-agnostic detection comparison on CA-1M and ScanNetV2 dataset. Point-based methods are not comparable on CA-1M, which can be attributed to closed-set training datasets and worse generalization to various objects. Our method is superior to both offline and online methods in CA-1M and performs the best on ScanNetV2 among the online methods. While scanNetV2 only provides ground-truth labels for common objects (18 categories), open-vocabulary methods detect many more objects, resulting in lower performance compared to offline point-based methods. Note that OnlineAnySeg segments images in an offline manner, and FPS is reported for the online fusion.

Method	AP_{15}	AP_{25}
No SA	16.85	14.23
No CA	34.55	28.16
No MVF	29.03	25.17
Ours	35.49	28.31

Table 2. Ablation studies of different modules proposed in our method on six scenes of CA-1M and eight scenes of ScanNetV2.

nificant improvement, 20.47 and 9.55 in AP_{25} compared to the best online method, illustrates that our method can detect objects effectively and accurately without the need for dense reconstruction, which is a significant advantage over other methods. Note that the FPS of OnlineAnySeg [31] is only for the fusion stage, and the segmentation of images is pre-processed, which is time-consuming. Our FPS is over 20 on average on the two datasets, and can detect and obtain the open-vocabulary semantic features or categories in real time.

4.3. Qualitative Results

As shown in Figure 5, we compare the detections of our methods to other state-of-the-art baselines. The background of our method is semi-transparent, since we do not rely on reconstruction for detection, which is adopted for all the other methods. On the first two rows, a comparison of two sequences of the CA-1M dataset is displayed, where the ground-truth is more fine-grained than ScanNetV2. Our method stands out as the best with detailed and accurate object detections. FCAF [28] is trained on closed-set datasets, which can detect the common objects (e.g., sofas and tables) accurately but struggle to detect the fine-grained objects (e.g., newspapers on the coffee table). SpatialLM [32]

Table 3. Comparison of run-time system FPS and GPU memory usage (GPU mem. for short) on the ScanNetV2 dataset. Our method (without dense reconstruction) is the most efficient and accurate online method.

Method	$AP_{15} \uparrow$	$AP_{25} \uparrow$	FPS \uparrow	GPU mem. \downarrow
EmbodiedSAM	5.22	2.46	10	12.5G
OnlineAnySeg	31.39	21.81	15	21.1G
Ours	37.46	31.36	20	7.0G

can only detect the big objects accurately, and there is a significantly high rate of missed detection. OnlineAnySeg [31] can successfully detect both the common objects and previously unseen objects thanks to the VFM. However, it is hard for OnlineAnySeg to detect the small but important objects (e.g., books and keys at the upper right of the first row). This can be attributed to the merging strategies that rely on point clouds for spatial overlaps, which may fail due to the noise or error in the reconstruction. In contrast, our method is reconstruction-free and leverages the rich context in multi-view images to detect and fuse the bounding boxes of 3D objects, leading to fine-grained and accurate 3D object detection.

As shown in Figure 6, our method is open-vocabulary and supports object retrieval with user-specific text prompts. For example, if the text prompt indicates it needs to charge the phone (first row in Figure 6), the power outlet on the wall marked by the red rectangle is highlighted to correspond to the prompt. This means that our method can be easily adapted to many downstream embodied tasks.

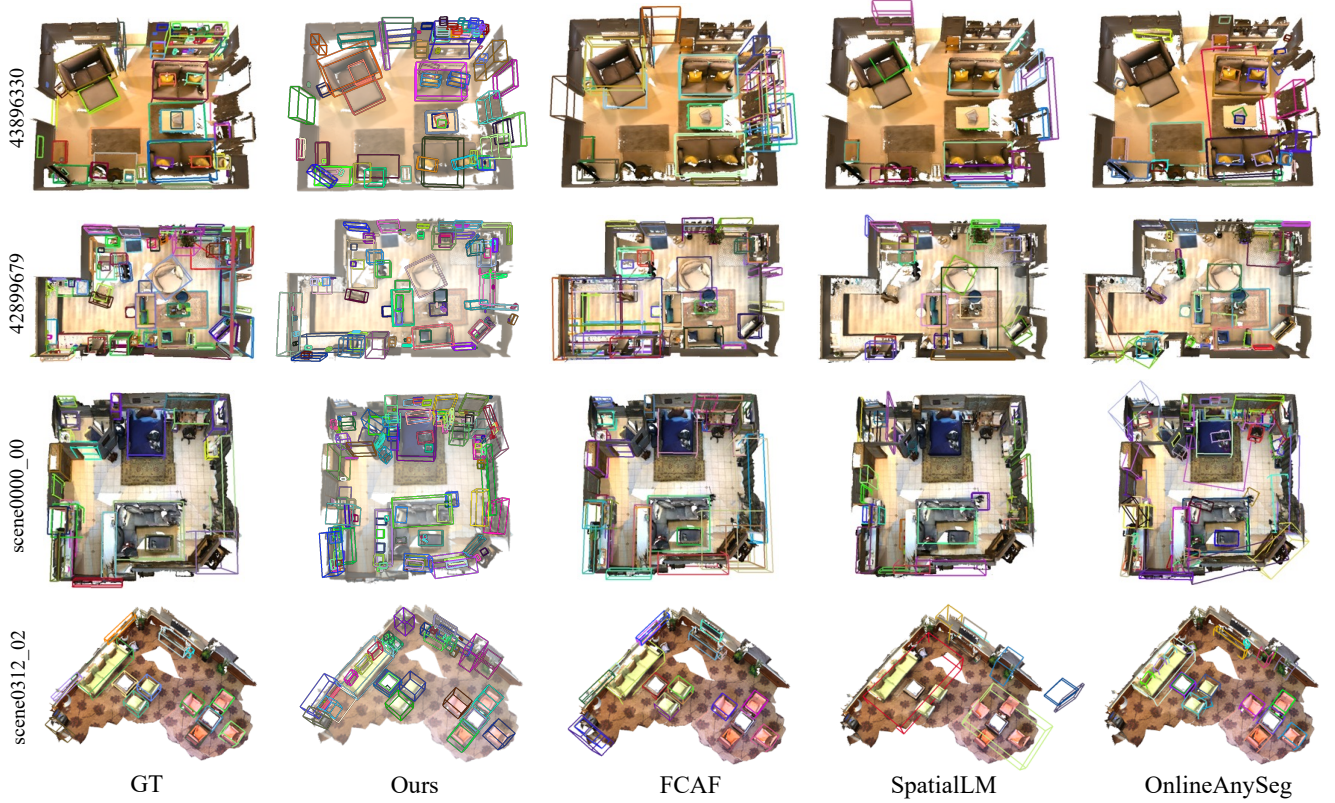


Figure 5. Gallery of 3D object detection on CA-1M and ScanNetV2. Our method is reconstruction-free, and the mesh is semi-transparent. Our method can accurately detect both the common objects and the objects that are not included in most closed-set datasets. Offline methods show poor generalization on fine-grained objects, and OnlineAnySeg (represented as the online method) is slightly better than offline methods but still has a high rate of missed detection. Best view on screen.

4.4. Ablation Studies

We mainly evaluate the proposed modules, including the spatial association (SA for short), correspondence association (CA for short), and the multi-view box fusion (MVF for short).

- SA: Without the SA module, the AP_{15} drops by 18.64, which indicates that the spatial association is important for global 3D object detection. It can provide spatially overlapping details to associate box proposals from different views.
- CA: The box correspondence module is mainly leveraged to associate small objects, and is necessary to provide accurate association to benefit the multi-view box fusion.
- MVF: The proposed multi-view box fusion is utilized to generate consistent 3D bounding boxes based on the association modules, leading to significant improvement in AP_{15} and AP_{25} compared to not using the MVF module.

As shown in Table 2, the ablation studies are performed on CA-1M and ScanNetV2. The proposed modules are beneficial to each other. Therefore, the full method is able to efficiently associate the box proposals and fuse them into

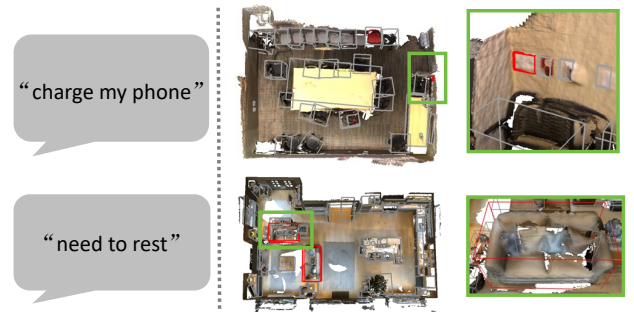


Figure 6. Open-vocabulary object retrieval with user-specific text prompts. Mesh is only for visualization.

globally consistent boxes.

4.5. Run-time and Memory Analysis

The core idea of our method is to perform real-time 3D object detection without dense reconstruction. Therefore, it is of great significance to compare our method with other alternatives in terms of running efficiency and memory usage.

As shown in Table 3, our method achieves the best performance in terms of both running time and memory usage. The GPU memory usage of our method is 7.0GB, which is much lower than that of online methods (12.5GB for embodiedSAM [37] and 21.1GB for OnlineAnySeg [31]). Our system FPS is over 20 on average. The main reason for the efficiency of our method is twofold. Firstly, it does not require dense reconstruction, which is a time-consuming process. Instead, it directly detects objects from RGB-D images. Secondly, the proposed random optimization based on particle filtering using pre-sampled swarm templates is highly efficient for online box fusion.

5. Conclusions

In conclusion, we introduce a novel reconstruction-free approach enabling efficient, real-time open-vocabulary 3D object detection. Compared to prior methods leveraging point cloud as the key 3D representation that is computationally expensive, our method employs pre-trained models, Cubify Anything for single-view detection, and CLIP for semantics given streaming RGB-D input. Multi-view predictions are associated via 3D NMS and 2D box correspondence, followed by an IoU-guided random optimization for consistent multi-view box fusion with minimal overhead. Evaluations on CA-1M and ScanNetV2 demonstrate the state-of-the-art performance of our method compared to other online approaches, which validates the novel paradigm for online 3D object detection.

References

- [1] Garrick Brazil, Abhinav Kumar, Julian Straub, Nikhila Ravi, Justin Johnson, and Georgia Gkioxari. Omni3d: A large benchmark and model for 3d object detection in the wild. In *Proceedings of the IEEE/CVF conference on computer vision and pattern recognition*, pages 13154–13164, 2023. 2, 6
- [2] Yihan Cao, Jiazhao Zhang, Zhinan Yu, Shuzhen Liu, Zheng Qin, Qin Zou, Bo Du, and Kai Xu. Cognav: Cognitive process modeling for object goal navigation with llms. *arXiv preprint arXiv:2412.10439*, 2024. 1
- [3] Jintai Chen, Biwen Lei, Qingyu Song, Haochao Ying, Danny Z Chen, and Jian Wu. A hierarchical graph network for 3d object detection on point clouds. In *Proceedings of the IEEE/CVF conference on computer vision and pattern recognition*, pages 392–401, 2020. 2
- [4] Angela Dai, Angel X Chang, Manolis Savva, Maciej Halber, Thomas Funkhouser, and Matthias Nießner. Scannet: Richly-annotated 3d reconstructions of indoor scenes. In *Proceedings of the IEEE conference on computer vision and pattern recognition*, pages 5828–5839, 2017. 6
- [5] Yao Duan, Chenyang Zhu, Yuqing Lan, Renjiao Yi, Xinwang Liu, and Kai Xu. Disarm: Displacement aware relation module for 3d detection. In *Proceedings of the IEEE/CVF Conference on Computer Vision and Pattern Recognition*, pages 16980–16989, 2022. 2
- [6] Francis Engelmann, Martin Bokeloh, Alireza Fathi, Bastian Leibe, and Matthias Nießner. 3d-mpa: Multi-proposal aggregation for 3d semantic instance segmentation. In *Proceedings of the IEEE/CVF conference on computer vision and pattern recognition*, pages 9031–9040, 2020. 2
- [7] Rui Huang, Henry Zheng, Yan Wang, Zhuofan Xia, Marco Pavone, and Gao Huang. Training an open-vocabulary monocular 3d detection model without 3d data. *Advances in Neural Information Processing Systems*, 37:72145–72169, 2024. 2
- [8] Chunlin Ji, Yangyang Zhang, Mengmeng Tong, and Shengxiang Yang. Particle filter with swarm move for optimization. In *International Conference on Parallel Problem Solving from Nature*, pages 909–918. Springer, 2008. 6
- [9] Li Jiang, Shaoshuai Shi, and Bernt Schiele. Open-vocabulary 3d semantic segmentation with foundation models. In *Proceedings of the IEEE/CVF Conference on Computer Vision and Pattern Recognition*, pages 21284–21294, 2024. 1
- [10] Alexander Kirillov, Eric Mintun, Nikhila Ravi, Hanzi Mao, Chloe Rolland, Laura Gustafson, Tete Xiao, Spencer Whitehead, Alexander C Berg, Wan-Yen Lo, et al. Segment anything. In *Proceedings of the IEEE/CVF International Conference on Computer Vision*, pages 4015–4026, 2023. 2, 3
- [11] Andreas Klöckner, Nicolas Pinto, Yunsup Lee, Bryan Catanzaro, Paul Ivanov, and Ahmed Fasih. Pycuda and pyopencl: A scripting-based approach to gpu run-time code generation. *Parallel computing*, 38(3):157–174, 2012. 6
- [12] Sebastian Koch, Narunas Vaskevicius, Mirco Colosi, Pedro Hermosilla, and Timo Ropinski. Open3dsd: Open-vocabulary 3d scene graphs from point clouds with queryable objects and open-set relationships. In *Proceedings of the IEEE/CVF Conference on Computer Vision and Pattern Recognition*, pages 14183–14193, 2024. 1
- [13] Yuqing Lan, Yao Duan, Chenyi Liu, Chenyang Zhu, Yueshan Xiong, Hui Huang, and Kai Xu. Arm3d: Attention-based relation module for indoor 3d object detection. *Computational Visual Media*, 8(3):395–414, 2022. 2
- [14] Justin Lazarow, David Griffiths, Gefen Kohavi, Francisco Crespo, and Afshin Dehghan. Cubify anything: Scaling indoor 3d object detection. *arXiv preprint arXiv:2412.04458*, 2024. 2, 3, 4, 5, 6
- [15] Seungjae Lee, Hyungtae Lim, and Hyun Myung. Patchwork++: Fast and robust ground segmentation solving partial under-segmentation using 3D point cloud. In *Proc. IEEE/RSJ Int. Conf. Intell. Robots Syst.*, pages 13276–13283, 2022. 6
- [16] Vincent Leroy, Yohann Cabon, and Jérôme Revaud. Grounding image matching in 3d with mast3r. In *European Conference on Computer Vision*, pages 71–91. Springer, 2024. 5
- [17] Haotong Lin, Sida Peng, Jingxiao Chen, Songyou Peng, Jiaming Sun, Minghuan Liu, Hujun Bao, Jiashi Feng, Xiaowei Zhou, and Bingyi Kang. Prompting depth anything for 4k resolution accurate metric depth estimation. 2024. 1
- [18] Tsung-Yi Lin, Michael Maire, Serge Belongie, James Hays, Pietro Perona, Deva Ramanan, Piotr Dollár, and C Lawrence Zitnick. Microsoft coco: Common objects in context. In *Computer vision—ECCV 2014: 13th European conference*,

- zurich, Switzerland, September 6-12, 2014, proceedings, part v 13, pages 740–755. Springer, 2014. 6
- [19] Shilong Liu, Zhaoyang Zeng, Tianhe Ren, Feng Li, Hao Zhang, Jie Yang, Qing Jiang, Chunyuan Li, Jianwei Yang, Hang Su, et al. Grounding dino: Marrying dino with grounded pre-training for open-set object detection. In *European Conference on Computer Vision*, pages 38–55. Springer, 2024. 2
- [20] Ze Liu, Zheng Zhang, Yue Cao, Han Hu, and Xin Tong. Group-free 3d object detection via transformers. In *Proceedings of the IEEE/CVF international conference on computer vision*, pages 2949–2958, 2021. 2, 4
- [21] Yuheng Lu, Chenfeng Xu, Xiaobao Wei, Xiaodong Xie, Masayoshi Tomizuka, Kurt Keutzer, and Shanghang Zhang. Open-vocabulary point-cloud object detection without 3d annotation. In *Proceedings of the IEEE/CVF conference on computer vision and pattern recognition*, pages 1190–1199, 2023. 2
- [22] Bohao Peng, Xiaoyang Wu, Li Jiang, Yukang Chen, Hengshuang Zhao, Zhuotao Tian, and Jiaya Jia. Oa-cnns: Omni-adaptive sparse cnns for 3d semantic segmentation. In *Proceedings of the IEEE/CVF Conference on Computer Vision and Pattern Recognition*, pages 21305–21315, 2024. 1
- [23] Charles R Qi, Hao Su, Kaichun Mo, and Leonidas J Guibas. Pointnet: Deep learning on point sets for 3d classification and segmentation. In *Proceedings of the IEEE conference on computer vision and pattern recognition*, pages 652–660, 2017. 2
- [24] Charles R Qi, Or Litany, Kaiming He, and Leonidas J Guibas. Deep hough voting for 3d object detection in point clouds. In *proceedings of the IEEE/CVF International Conference on Computer Vision*, pages 9277–9286, 2019. 1, 2, 4, 6
- [25] Charles R Qi, Xinlei Chen, Or Litany, and Leonidas J Guibas. Invotenet: Boosting 3d object detection in point clouds with image votes. In *Proceedings of the IEEE/CVF conference on computer vision and pattern recognition*, pages 4404–4413, 2020. 2
- [26] Lu Qi, Jason Kuen, Tiancheng Shen, Jiuxiang Gu, Wenbo Li, Weidong Guo, Jiaya Jia, Zhe Lin, and Ming-Hsuan Yang. High quality entity segmentation. In *2023 IEEE/CVF International Conference on Computer Vision (ICCV)*, pages 4024–4033. IEEE, 2023. 3
- [27] Alec Radford, Jong Wook Kim, Chris Hallacy, Aditya Ramesh, Gabriel Goh, Sandhini Agarwal, Girish Sastry, Amanda Askell, Pamela Mishkin, Jack Clark, et al. Learning transferable visual models from natural language supervision. In *International conference on machine learning*, pages 8748–8763. PMLR, 2021. 2, 4
- [28] Danila Rukhovich, Anna Vorontsova, and Anton Konushin. Fcaf3d: Fully convolutional anchor-free 3d object detection. In *European Conference on Computer Vision*, pages 477–493. Springer, 2022. 1, 2, 6, 7
- [29] Danila Rukhovich, Anna Vorontsova, and Anton Konushin. Tr3d: Towards real-time indoor 3d object detection. In *2023 IEEE International Conference on Image Processing (ICIP)*, pages 281–285. IEEE, 2023. 1, 2, 6, 7
- [30] Nur Muhammad Mahi Shafiullah, Chris Paxton, Lerrel Pinto, Soumith Chintala, and Arthur Szlam. Clip-fields: Weakly supervised semantic fields for robotic memory. *arXiv preprint arXiv:2210.05663*, 2022. 2
- [31] Yijie Tang, Jiazhao Zhang, Yuqing Lan, Yulan Guo, Dezun Dong, Chenyang Zhu, and Kai Xu. Onlineanyseg: On-line zero-shot 3d segmentation by visual foundation model guided 2d mask merging. *arXiv preprint arXiv:2503.01309*, 2025. 2, 3, 4, 6, 7, 9
- [32] ManyCore Research Team. Spatiallm: Large language model for spatial understanding. <https://github.com/manycore-research/SpatialLM>, 2025. 3, 6, 7
- [33] Jintao Wang, Zuyi Zhao, Jiayi Qu, and Xingguo Chen. Appa-3d: an autonomous 3d path planning algorithm for uavs in unknown complex environments. *Scientific Reports*, 14(1): 1231, 2024. 1
- [34] Shuzhe Wang, Vincent Leroy, Yohann Cabon, Boris Chidlovskii, and Jerome Revaud. Dust3r: Geometric 3d vision made easy. In *Proceedings of the IEEE/CVF Conference on Computer Vision and Pattern Recognition*, pages 20697–20709, 2024. 5
- [35] Zhenyu Wang, Yali Li, Taichi Liu, Hengshuang Zhao, and Shengjin Wang. Ov-uni3detr: Towards unified open-vocabulary 3d object detection via cycle-modality propagation. In *European Conference on Computer Vision*, pages 73–89. Springer, 2024. 2
- [36] Qian Xie, Yu-Kun Lai, Jing Wu, Zhoutao Wang, Yiming Zhang, Kai Xu, and Jun Wang. Mlcvnet: Multi-level context votenet for 3d object detection. In *Proceedings of the IEEE/CVF conference on computer vision and pattern recognition*, pages 10447–10456, 2020. 2
- [37] Xiuwei Xu, Huangxing Chen, Linqing Zhao, Ziwei Wang, Jie Zhou, and Jiwen Lu. Embodiedsam: Online segment any 3d thing in real time. *arXiv preprint arXiv:2408.11811*, 2024. 2, 3, 4, 6, 7, 9
- [38] Xiuwei Xu, Chong Xia, Ziwei Wang, Linqing Zhao, Yueqi Duan, Jie Zhou, and Jiwen Lu. Memory-based adapters for online 3d scene perception. In *Proceedings of the IEEE/CVF Conference on Computer Vision and Pattern Recognition*, pages 21604–21613, 2024. 2, 3
- [39] Sixu Yan, Zeyu Zhang, Muzhi Han, Zaijin Wang, Qi Xie, Zhitian Li, Zhehan Li, Hangxin Liu, Xinggang Wang, and Song-Chun Zhu. M 2 diffuser: Diffusion-based trajectory optimization for mobile manipulation in 3d scenes. *IEEE Transactions on Pattern Analysis and Machine Intelligence*, 2025. 1
- [40] Lihe Yang, Bingyi Kang, Zilong Huang, Xiaogang Xu, Jiashi Feng, and Hengshuang Zhao. Depth anything: Unleashing the power of large-scale unlabeled data. In *Proceedings of the IEEE/CVF Conference on Computer Vision and Pattern Recognition*, pages 10371–10381, 2024. 1
- [41] Yunhan Yang, Xiaoyang Wu, Tong He, Hengshuang Zhao, and Xihui Liu. Sam3d: Segment anything in 3d scenes. *arXiv preprint arXiv:2306.03908*, 2023. 3
- [42] Hang Yin, Xiuwei Xu, Zhenyu Wu, Jie Zhou, and Jiwen Lu. Sg-nav: Online 3d scene graph prompting for llm-based

- zero-shot object navigation. *Advances in Neural Information Processing Systems*, 37:5285–5307, 2024. [1](#)
- [43] Hanxue Zhang, Haoran Jiang, Qingsong Yao, Yanan Sun, Renrui Zhang, Hao Zhao, Hongyang Li, Hongzi Zhu, and Zetong Yang. Detect anything 3d in the wild. *arXiv preprint arXiv:2504.07958*, 2025. [3](#)
- [44] Jiazhao Zhang, Chenyang Zhu, Lintao Zheng, and Kai Xu. Rosefusion: random optimization for online dense reconstruction under fast camera motion. *ACM Transactions on Graphics (TOG)*, 40(4):1–17, 2021. [4](#), [6](#)
- [45] Jiazhao Zhang, Nandiraju Gireesh, Jilong Wang, Xiaomeng Fang, Chaoyi Xu, Weiguang Chen, Liu Dai, and He Wang. Gamma: Graspability-aware mobile manipulation policy learning based on online grasping pose fusion. In *2024 IEEE International Conference on Robotics and Automation (ICRA)*, pages 1399–1405. IEEE, 2024. [1](#)
- [46] Gengze Zhou, Yicong Hong, and Qi Wu. Navgpt: Explicit reasoning in vision-and-language navigation with large language models. In *Proceedings of the AAAI Conference on Artificial Intelligence*, pages 7641–7649, 2024. [1](#)
- [47] Yin Zhou and Oncel Tuzel. Voxelnet: End-to-end learning for point cloud based 3d object detection. In *Proceedings of the IEEE conference on computer vision and pattern recognition*, pages 4490–4499, 2018. [1](#), [2](#)